

ATLAS NSW Alignment System

Study on Inductors

Senior Thesis

Presented to Faculty of the School of Arts and Sciences
Brandeis University

Undergraduate Program in Physics

by

Cheng Li

Advisor:

James Bensinger

Waltham, MA, Dec 2017

Signatures

James Bensinger Ph.D., Committee Member

Date

Richard Fell Ph.D., Committee Member

Date

Acknowledgements

I would like to thank my thesis advisor, James Bensinger, for his constant support throughout this project. I would also like to thank Kevan Hashemi and Richard Studley for their mentorship and leadership in the HEP Lab. And I would like to thank all my colleagues in the HEP Lab for their help in the project.

Abstract

Brandeis University High Energy Physics Group is working on the alignment system of the New Small Wheel (NSW) for the ATLAS upgrade project. The Disk Shielding (JD) of the NSW will be exposed in a strong magnetic field and so do the light source (contact injectors) that will be installed on the JD. This paper will describe the effect of the magnetic field on the inductors in contact injectors. This paper will also show that the current design of the layout of injectors will prevent the injectors from being significantly affected by the magnetic field.

1. Background

1.1. ATLAS

Large Hadron Collider, or LHC, at CERN is the world's largest and most powerful particle accelerator. ATLAS and CMS are the two general-purpose detectors at the LHC. [1] The LHC is undergoing an upgrade to supply a luminosity of $5 * 10^{34} \text{ cm}^{-2} \text{ s}^{-1}$. [2] To cope with the corresponding time increase, the ATLAS detector needs to be upgraded. The largest phase-1 upgrade project for the ATLAS Muon System is the replacement of the present first station in the forward regions with the New Small Wheel, to be installed during the LHC long shutdown in 2018/19. [3] Brandeis High Energy Physics (HEP) group focuses on designing and building the alignment system for the NSW, and the subject of my study is the light source, contact injector. Contact injectors will be installed on the Disk Shielding (JD), which supports the muon chambers in the NSW, shields these chambers from radiation and returns the magnetic field from the solenoid magnet in a well-defined way. [4]

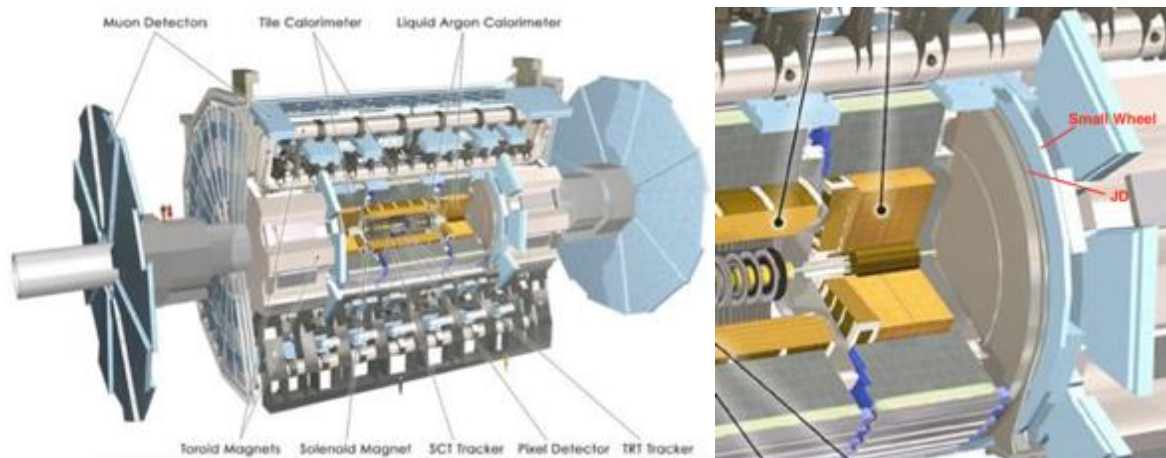


Fig1. ATLAS (left); Close-up of the New Small Wheel and JD (right)

1.2. Alignment System

The alignment system is designed to create a coordinate system that can be incorporated with the ATLAS and LHC coordinate systems and to know the location and shape of the chambers in the muon spectrometer.

The current end-cap optical system is an absolute alignment system, meaning that the sensors provide the muon chamber positions at any given time without any external input. The optical system of the NSW should follow the same principle, i.e. it should also be an absolute system. The optical absolute alignment system of the end-caps is designed such that the positions with respect to each other in the precision coordinate of any three chambers that can be traversed by a muon track can be determined with an accuracy of $40\ \mu\text{m}$. The key prerequisite for an absolute alignment system is a knowledge at a level of typically $20\ \mu\text{m}$ and $50\ \mu\text{rad}$ of the positions and rotations of the optical sensor elements (CCDs, lenses, light sources) with respect to the active detector elements (wires, strips, etc.) of the chamber they are mounted on, i.e. their positions and rotations in the local chamber coordinate system.

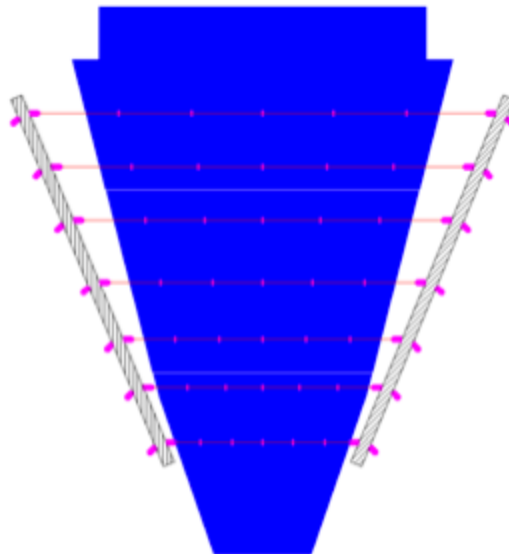


Fig2. Layout in the option with light sources on the chambers, integrating chamber-to-bar alignment with chamber deformation monitoring.

For linking quadruplets to alignment bars, presumably the easiest solution are cameras on alignment bars viewing targets (point-like light sources, e.g. laser diodes, or RASNIK masks) mounted for instance, but not necessarily, near the four quadruplet corners, either on the quadruplet surface or on the side faces. Cameras on bars of large sectors view targets on small

chambers, and cameras on bars of small sectors view targets on large chambers (Fig2), by which the position of the alignment bars and muon chambers can be determined. The light source on the muon chambers is provided by the contact injector circuit.

1.3. Contact Injector

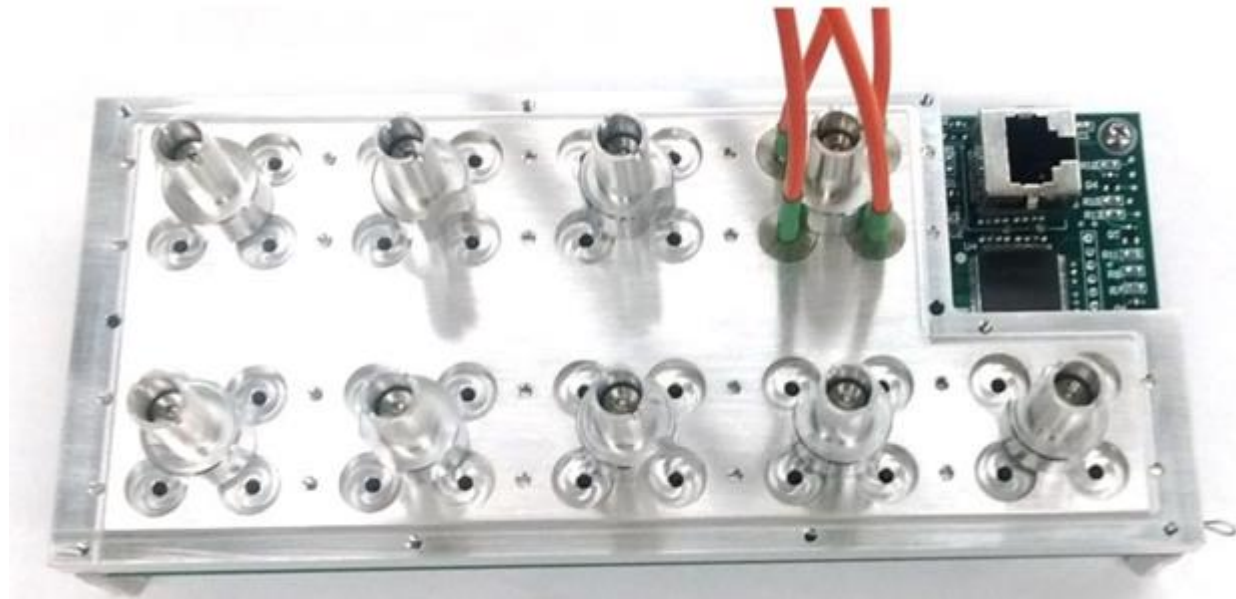


Fig3. Thirty-Six Way Contact Injector with Fiber Mounting Plate

The Contact Injector (A2080) is a LWDAQ device that provides light sources coupled into optical fibers by contact injection. The other end of the optic fibers will be mounted on source plates mounted on the chambers for the optical system. The A2080A provides 36 separate, individually-fused buck converters to power 36 deep-red Luxeon Z LEDs, by converting the LWDAQ $\pm 15\text{V}$ power supply into an LED drive supply. The LED drive voltage is equal to the forward voltage drop of the selected LED plus a small voltage across a $0.1\text{-}\Omega$ current sensing resistor. The A2080 is equipped with deep-red LXZ1-PA01 LEDs and the forward voltage drop is around 2.1 V at 800 mA. [5] The LEDs are positioned right below the holes on the fiber mounting plate and eject light through the fiber to the muon chambers.

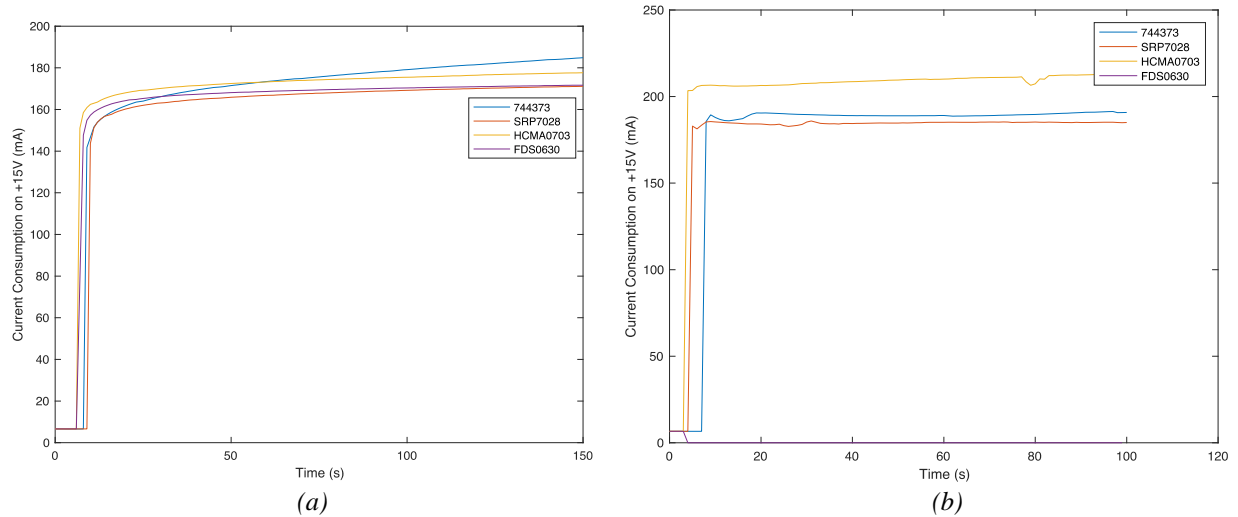


Fig5. Current drawn into buck converter circuits with different inductors. (a): no magnetic field applied on the inductors; (b): a 0.45T magnetic field applied on the inductors.

In Fig5, the current drawn into the circuit with inductor HCMA0703 increased significantly and the fuse of the circuit with inductor FDS0630 blew up when the external magnetic field was applied. Based on this test, we rejected these two inductors. The current in the circuits with inductors 744373 and SRP7028 was similar with and without the external magnetic field. Therefore, I conducted further experiments to decide the inductor to be used on the injector circuit.

3. Experiments on Inductors

3.1. Inductance Versus Magnetic Field Strength

We wanted to find out how the inductance of the inductor used in the buck converter changes with respect to an external magnetic field. Therefore, I made a separate circuit to measure the inductance of four different kinds of inductors: Inductor SRP7028, 744373, Iron Core Toroidal Inductor, Air Core Toroidal Inductor.

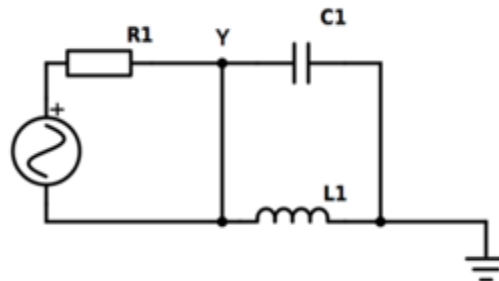


Fig6. Circuit for inductance measurement

When the input current is at the resonance frequency: $f_c = \frac{1}{2\pi\sqrt{LC}}$, the amplitude of voltage at point Y will reach its maximum. Therefore, by adjusting the input frequency and monitoring the voltage at point Y, we can read out the resonance frequency from the function generator and calculate the inductance. I used a micrometer stage to move the circuit into the magnetic field and kept measuring the inductance while the field strength was increasing.

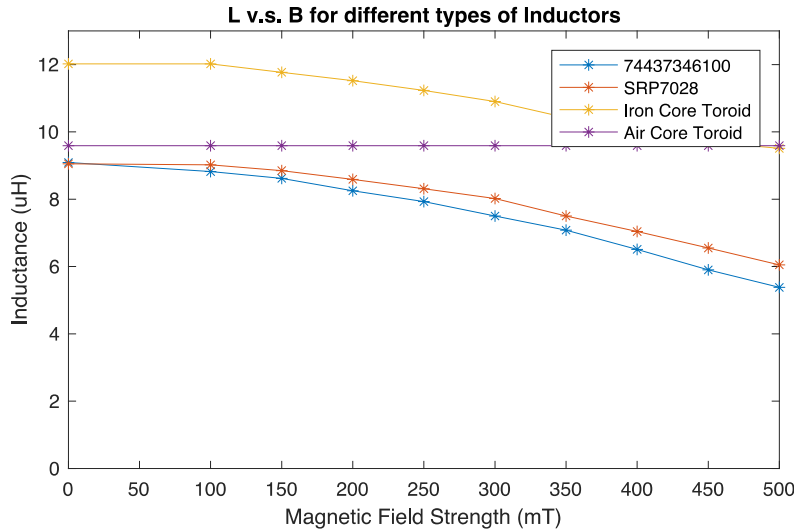


Fig7. The change of Inductance when the inductor is moving into the magnetic field

This graph shows that as the field strength increases, the inductance of the Air Core Toroidal Inductor remains the same while the inductance of other three inductors decreases. We conclude that the air core inductor is not affected by the external magnetic field; however, due to the space limit on the circuit board, we cannot use air core inductors on our circuit. Since the inductance of inductor SRP7028 changes less than inductor 744373, we chose to use it on our injectors for the NSW alignment system.

Then, in order to verify that the decrease of the inductance matches the increase of the current drawn into the buck converter, I plotted the graph of these two changes on the same graph:

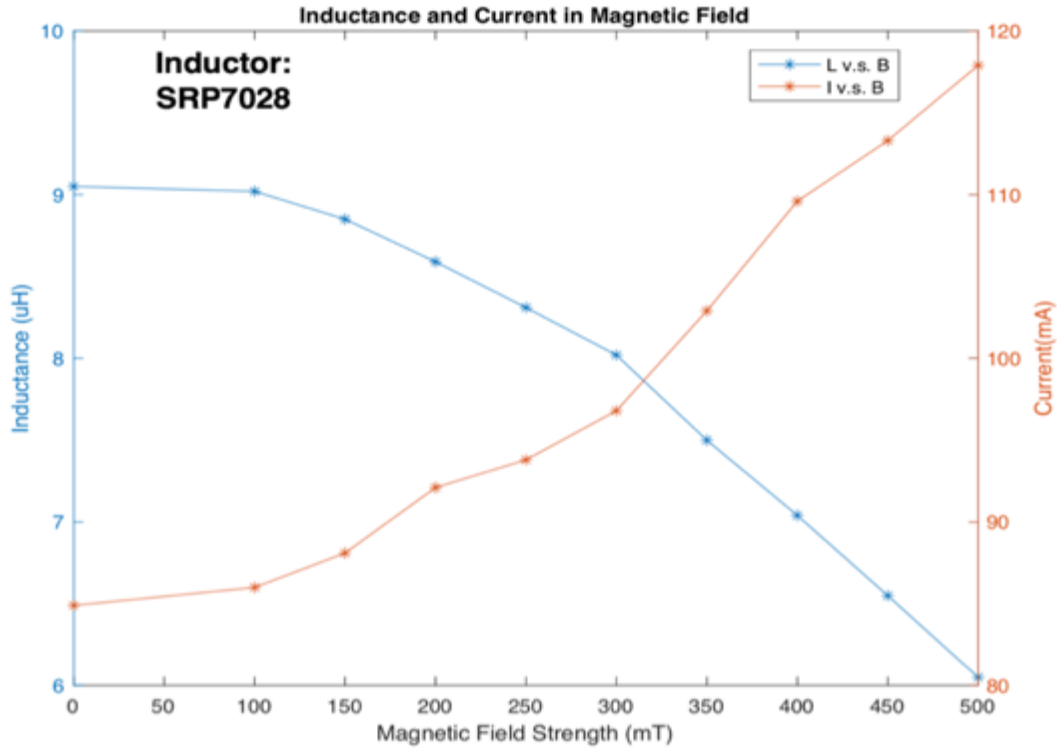


Fig8. This graph shows that the change of inductance and the change of current are related.

The current drawn into the buck converter is calculated by the charge time t_c multiplies the charge rate of the current $\frac{dI}{dt}$: $I_{max} = t_c \frac{dI}{dt}$. Then from the inductance equation $V = L \frac{dI}{dt}$, we have $I_{max} = t_c \frac{V}{L}$. Therefore, the current drawn into the buck converter should be proportional to the inverse of the inductance.

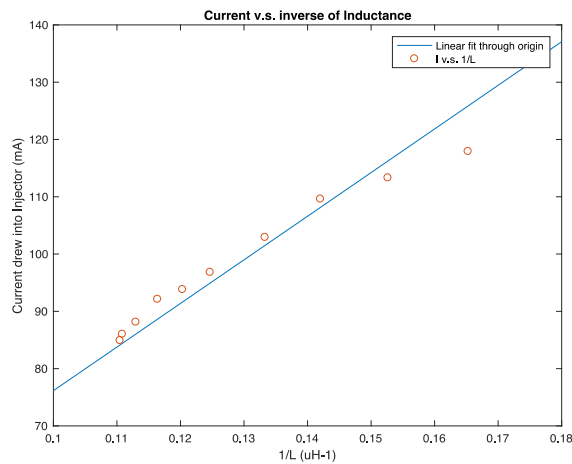


Fig9. Current v.s. inverse of Inductance

In Fig9, the straight line is a linear fit through the origin. From the graph, we can see that the current is indeed proportional to the inverse of the inductance, which verifies that the decrease in the inductance causes the increase of the current.

3.2. Inductance Versus the Orientation of Magnetic Field

We want to find out how the orientation of the magnetic field affects the inductance. In this experiment, I mounted the circuit for inductance measurement onto a rotation stage and placed the stage in a horseshoe magnet. The circuit board rotated along z-axis and I assumed that the magnetic field strength on the inductor remained the same during the measurement. With the axis of the inductor being parallel with the direction of the magnetic field as 0 degree, I rotated the board counter-clockwise and made measurements in 30-degree steps.

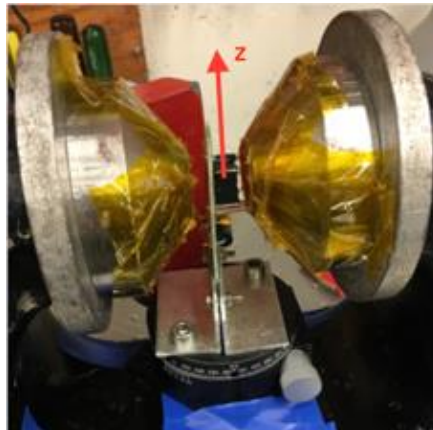


Fig10. Setup for rotation measurement.

By measuring the resonance frequency, I can calculate how the inductance changes with respect to the orientation of the magnetic field. I did this rotation measurement on the iron core toroidal inductor and the SRP7048, which is an iron core solenoidal inductor.

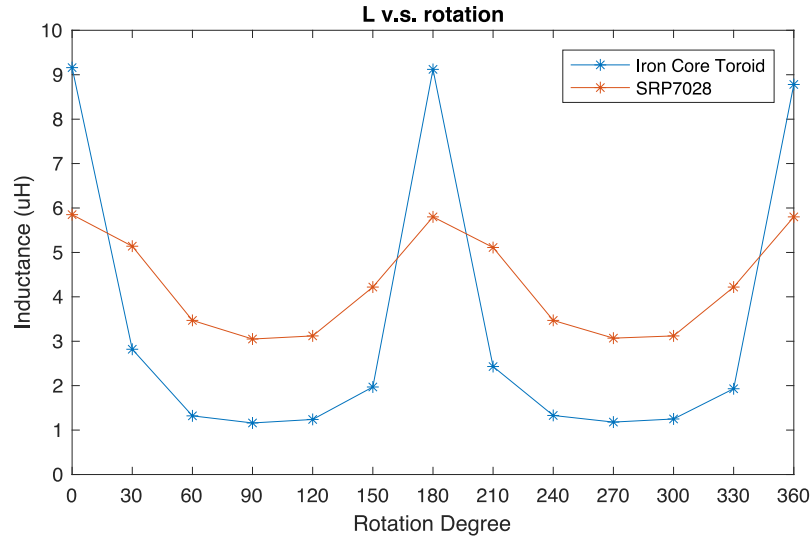


Fig11. Inductance v.s. orientation of the field

However, the initial assumption that the magnetic field on the inductor remained the same during the measurement was incorrect. Because the permeability of iron is larger than that of air and the gap between two iron poles is small, the field strength increases over 20% when the iron core toroid inductor is at 90/270 degree, comparing to when it is at 0/180 degree. However, this effect on the solenoid inductor is comparably smaller because the solenoid inductor is smaller in dimensions. Therefore, the inductance of the toroid inductor decreases more might be caused by the increase of the strength of the magnetic field, instead of the orientation.

In order to reduce the effect of the change of the magnetic field strength, I removed the iron poles on the magnetic and repeated the experiment. Since the air gap between the horseshoe magnet became much wider, the field changed less when the inductors were rotated.

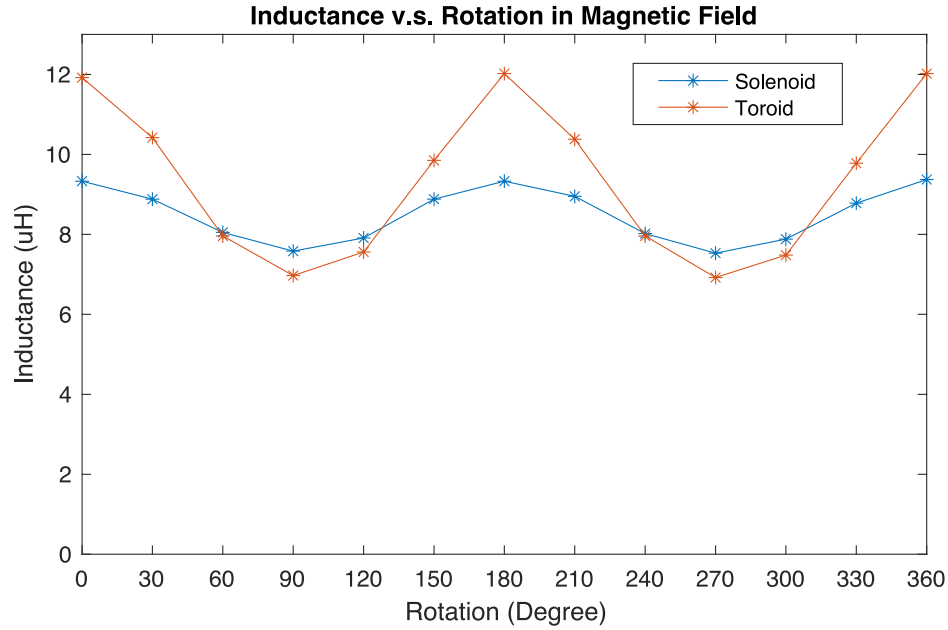
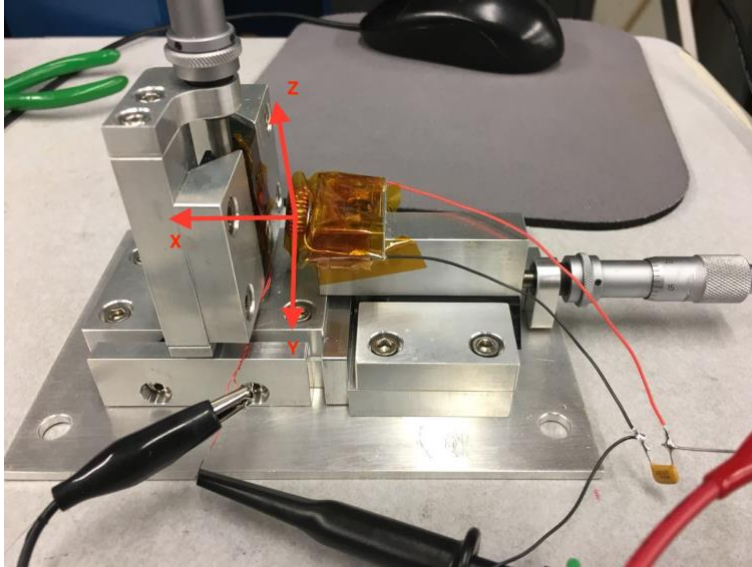


Fig12. Inductance v.s. orientation measurement without iron poles

Without the iron poles on the magnet, the field strength is 160 - 170 mT during the measurement of the toroid inductor and 155 - 160 mT during the measurement of the solenoid inductor. From the result in Fig7, we can see that 10 mT difference of the magnetic field strength will not cause the significant change of inductance shown in Fig12. Therefore, the orientation of the magnetic field must have caused the change of inductance and this effect is maximized when the axis of the inductor is perpendicular with the direction of the magnetic field.

3.3. The Leakage Field of Inductors

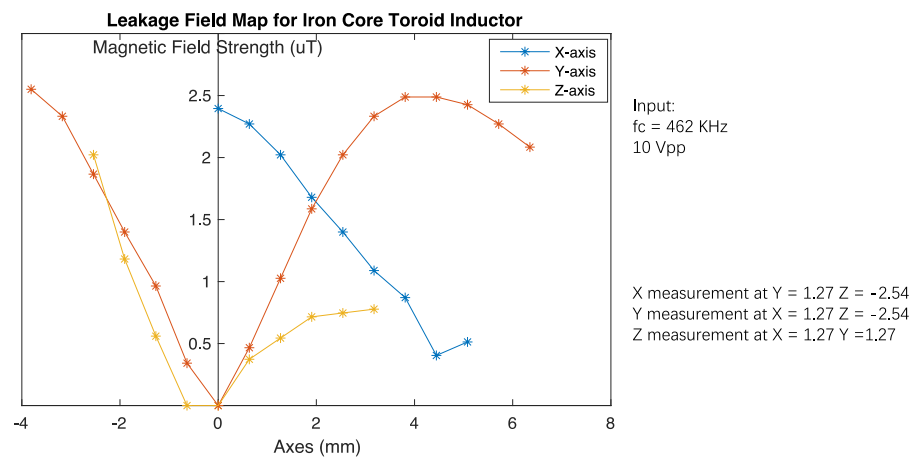
The Front-End cart at CERN has a DC-DC converter that converts a 12V input voltage to 1.2V. The converter contains a solenoidal inductor and an oscillator, which oscillates the current into the inductor at 1.7 MHz. Therefore, there is induced current on the stripes in the Front-End cart due to the leakage field of the inductor. This induced current becomes the noise in the Front-End measurement. In order to understand and solve this problem, I used following apparatus to measure the leakage field of a solenoid inductor and a toroid inductor.



Coil:
 10 turns
 8.4mm diameter

Fig13. Setup for leakage field measurement.

In this setup, the origin is at the center of the inductor, x direction is towards the coil and the y direction is coming out of the page. The inductor is connected in parallel with a capacitor and then connected in series with a resistor. A 10Vpp sinusoidal current at the resonance frequency of the inductor was applied to maximize the leakage field. Then, I used a pick-up coil to measure the leakage field by measuring the induced emf generated across the coil.



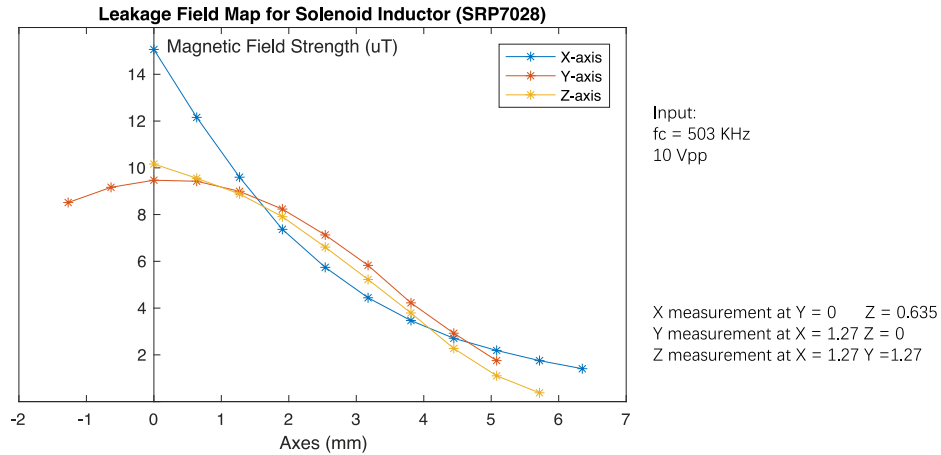


Fig14. Leakage Field Map for Two Inductors

In Fig14, the horizontal axis is the three axes of the micrometer stage. I fixed two axes position and changed the third axis to take measurements. We can see that with the same the amplitude and similar frequency (10% difference) of the input current, the leakage field of a solenoid inductor is much bigger than that of a toroid inductor.

4. Case Study

4.1. Injector Position

We want to make sure that the installation position of the contact injectors has the minimal magnetic field so that the inductors on the circuit are less affected. Therefore, I mapped out the magnetic field around the originally designated installation position of the injectors, where each square represents a contact injector and the arrow indicates the magnetic field direction at that point.

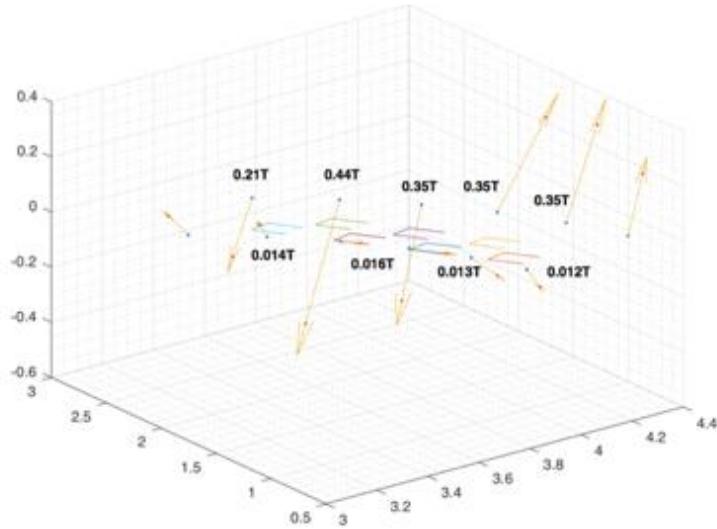


Fig15. Magnetic Field Map.

In the magnetic field map, there were three injectors close to a field over 0.4T, which would cause over 2uH decrease of the inductance and severely affect the performance of the injectors. Therefore, we decided to rearrange the location of the injectors so that all the injectors will be located in a position with weaker magnetic field.

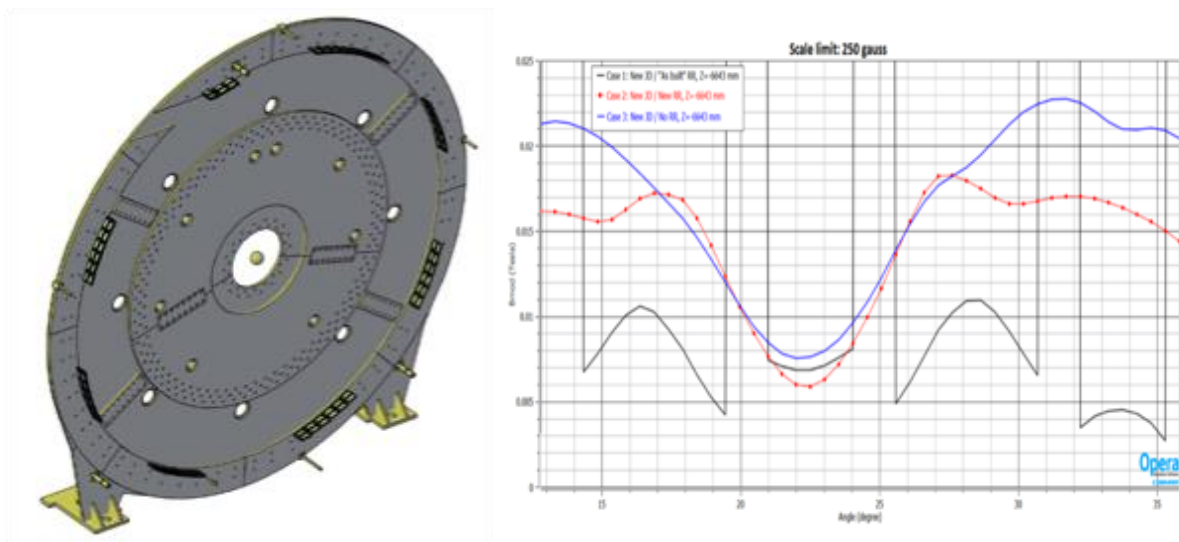


Fig16. New design for the injectors. Injector position (left), field map (right).

In the new setup, we moved the injectors away from the coil in the detector and stacked two layers of injectors so that they will all be away from the coils that generate the magnetic field on the JD. The magnetic field strength at the new injectors position is the blue line in the field map

in Fig16, and it is less than 25mT. Therefore, the influence of the external magnetic field will be trivial and injectors will perform as we expected.

4.2. Noise in Front-End Measurements

From the leakage field measurements in Section 3.3, the solenoid inductor generates much bigger leakage field than the toroid inductor in close range. One solution to the noise problem at Front-End is to replace solenoid inductors with toroid inductors. However, the dimension of the toroidal inductor is 15mm*15mm*7mm while the dimension of the solenoidal inductor is 7mm*7mm*3mm. Due to the limitation of space, we cannot use the toroidal inductor on the circuit.

But from Fig14., the leakage field generated by the solenoidal inductor drops dramatically when the pickup coil moves away from the inductor and becomes less than 2uT when the coil is 6mm away from the inductor. Therefore, if the solenoidal inductor were to be moved 6mm away from the instruments that are sensitive to magnetic field, the noise on the measurement would be reduced significantly.

5. Conclusion and Future Work

In this project, I focused on studying how magnetic fields influence inductors' inductance and how the change of inductance eventually results in the current consumption of the contact injectors used in ATLAS for the alignment system. Then I used this finding to help improve our design of the layout of the contact injectors. At the same time, the experiments on the leakage field of inductors also helped in proposing a solution to the problem at Front-End.

To further this project, I will try to find out why the inductors' inductance changes with respect to the orientation of a magnetic field. I am not able to propose any specific theory yet due to the limitation of project time and physics knowledge, but it will be worth working on in the future. And if the Front-End accepts my suggestion on the adjustment of the inductors, I can then verify whether the method is efficient in practice and make improvement base on the result.

Reference:

- [1] ATLAS Experiment, CERN Accelerating science,
<https://home.cern/about/experiments/atlas>.
- [2] A Zibell, “Micromegas Detectors for the Upgrade of the ATLAS Muon Spectrometer”,
IOPscience 9, 20 Aug. 2014, <http://iopscience.iop.org/article/10.1088/1748-0221/9/08/C08013/meta>.
- [3] Stelzer, Bernd. “The New Small Wheel Upgrade Project of the ATLAS Experiment”,
Nuclear and Particle Physics Proceedings, vol. 273-275, 2016, pp 1160-1165.
- [4] Hedberg, Vincent. The ATLAS Shielding Project,
<http://atlas.web.cern.ch/Atlas/GROUPS/Shielding/shielding.htm> - part6.
- [5] Hashemi, Kevan. “Contact Injector Manual”, *Brandeis University High Energy Physics Electronics Shop*, <http://alignment.hep.brandeis.edu/Electronics/A2080/M2080.html>.